IECMA 2024 Conference

The 2nd International Electronic Conference on Machines and Applications

18–20 June 2024 | Online

Silicon Carbide-Based Three-Phase Current Source Inverter: Simulation and Experimental Validation

Gaetano Turrisi , Luigi Danilo Tornello, Giuseppe Scarcella, Giacomo Scelba

University of Catania

Introduction

The main aim of this paper is to present the operational principle of this power converter, its modelling in a circuit-based simulation platform, and the results obtained from simulations and experimental tests conducted on a current source inverter equipped with 600V 20A SiC devices.

The following study investigated the traditional CSI topology with six switches. CSI power switches have the characteristic of allowing unidirectional current flow and requiring reverse blocking (RB) voltages. This last feature is therefore achieved by combining power switches in series with Schottky diodes, as shown in the figure below

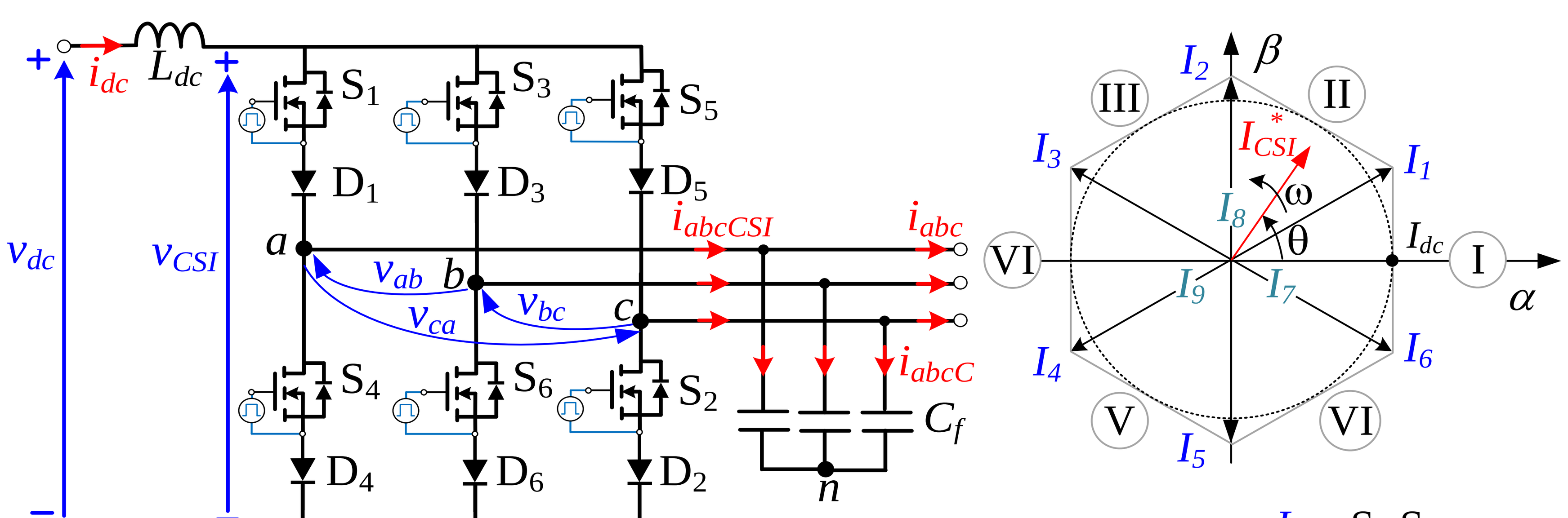

Modulation Strategy

A space vector modulation (SVM) switching scheme is implemented, where only two switches, one from the upper devices and the other from the lower devices, can conduct currents at the same time.

Active Vectors:
- I_1 S1 S2
- I_2 S2 S3
- I_3 S3 S4
- I_4 S4 S5
- I_5 S5 S6
- I_6 S6 S1

Null Vectors I_0:
- I_7 S1 S4 (I) (VI)
- I_8 S3 S6 (III) (VI)
- I_9 S5 S2 (II) (V)

The modified full wave symmetrical modulation (MFSM) switching sequence has been adopted:

$$I_0, I_{h+1}, I_h, I_{h+1}, I_0 \quad \text{for } h = 1,\ldots,5$$

$$I_0, I_1, I_{h,}, I_1, I_0 \quad \text{for } h = 6$$

where h is the sector number (h=1,…,6).

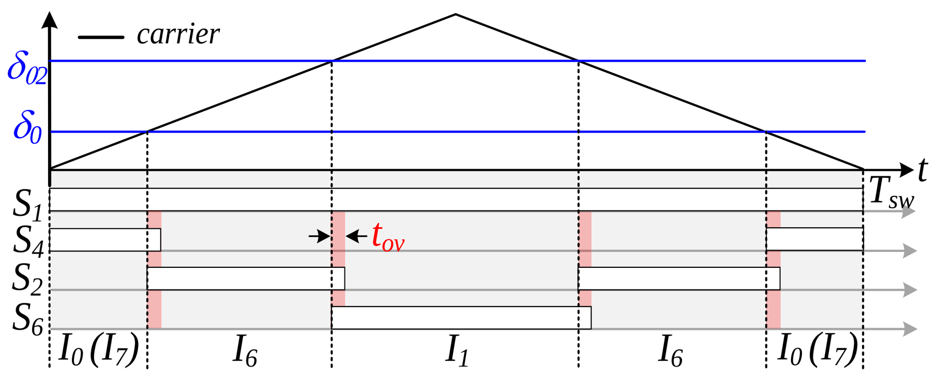

A scaled prototype of the CSI traction drive has been both modelled and experimentally validated

Modelling of the SiC CSI-Based Drive

The entire traction drive has been modelled in detail to assess the performance of the SiC CSI6-RB. This involved simulating the system by integrating LTspice models of power devices in the PSIM environment, allowing for an accurate replication of the power converter behaviour. The simulations employ the second-order trapezoidal integration method, with the smallest time step set to 10 ps. The switching frequency is fixed at *100 kHz*, and an overlap time t_{ov} of *400 ns* is applied

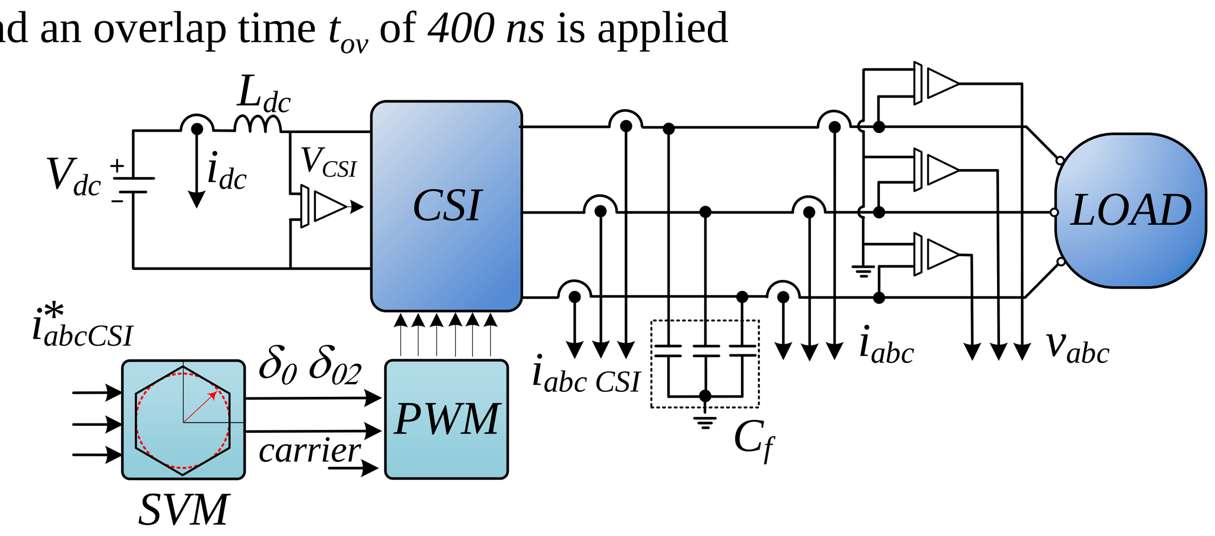

The transient analysis of SiC MOSFETs and Schottky diodes is performed by including in the SiC models the data provided by the manufacturer's datasheet, which includes all dynamic-state I-V and C-V characteristics.

Table I: CSI's passive components values.

DC-link inductor		Capacitor filter	
parameter	*value*	*parameter*	*value*
L_{dc}	1mH	C_f	3.3µF
R_{Ldc}	77mΩ	ESR_{Cf}	13.66mΩ

Table II: SiC-MOSFET specifications.

$V_{(BR)DS}$	650 V	R_{dsON}	78m Ω
I_{DS}	20 A		

Table III: Schottky Diode specifications.

$V_{(BR)D}$	650 V	$V_f\,(T_j$=150°C)	1.75 V
$I_D\,(T_j$=150°C)	20 A		

Table IV: Load parameters.

Test 1		Test 2	
R_{load}	47 Ω	R_{load}	131 Ω
		L_{load}	0.44 mH
PF	1	PF	0.73

Equivalent circuit of SiC MOSFET and SiC Schottky Diode.

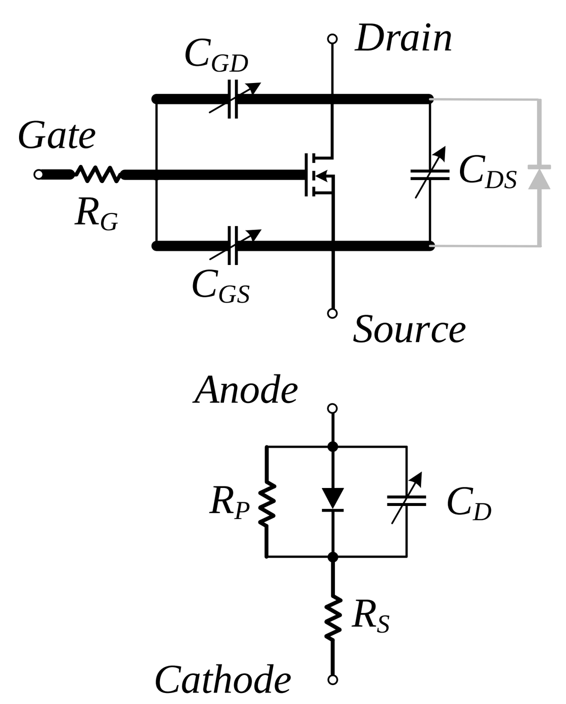

Experimental Investigation

The experimental test bench is shown. A dSPACE DS1006 has been used to implement the open-loop control and the field-programmable gate arrays (FPGAs) is used for the PMW signal generation. The experimental parameter are listed in Tabs I-IV. The switching frequency is set to 100kHz and the fundamental frequency of the output waveforms is 50Hz. A measurement campaign was conducted using a purely resistive load connected in a star configuration. The load was set to 47Ω, the modulation index was fixed to m_a=0.9 and a dc-link current of 4A was applied, regulated by a dedicated power supply with constant current functionality. A second test is performed with an RL load with PF=0.73.

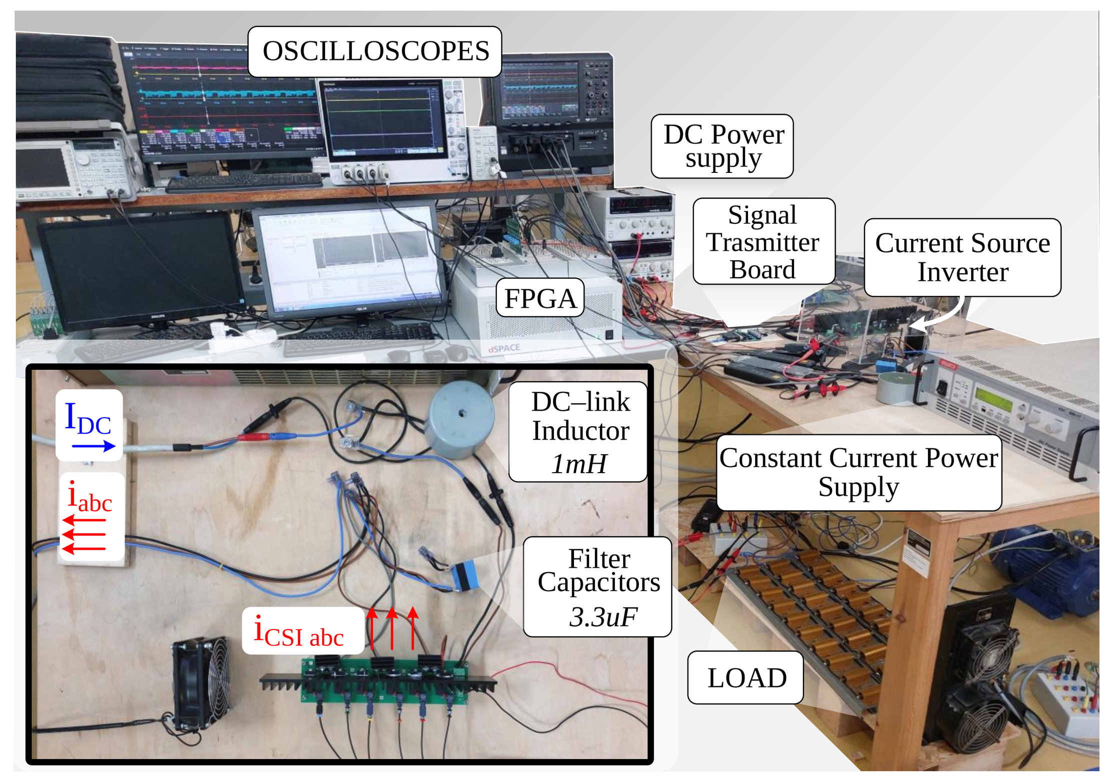

The purpose of this test is to display the experimental waveforms of the converter and verify the accuracy of the simulated system model.

CASE 1 – PF =1

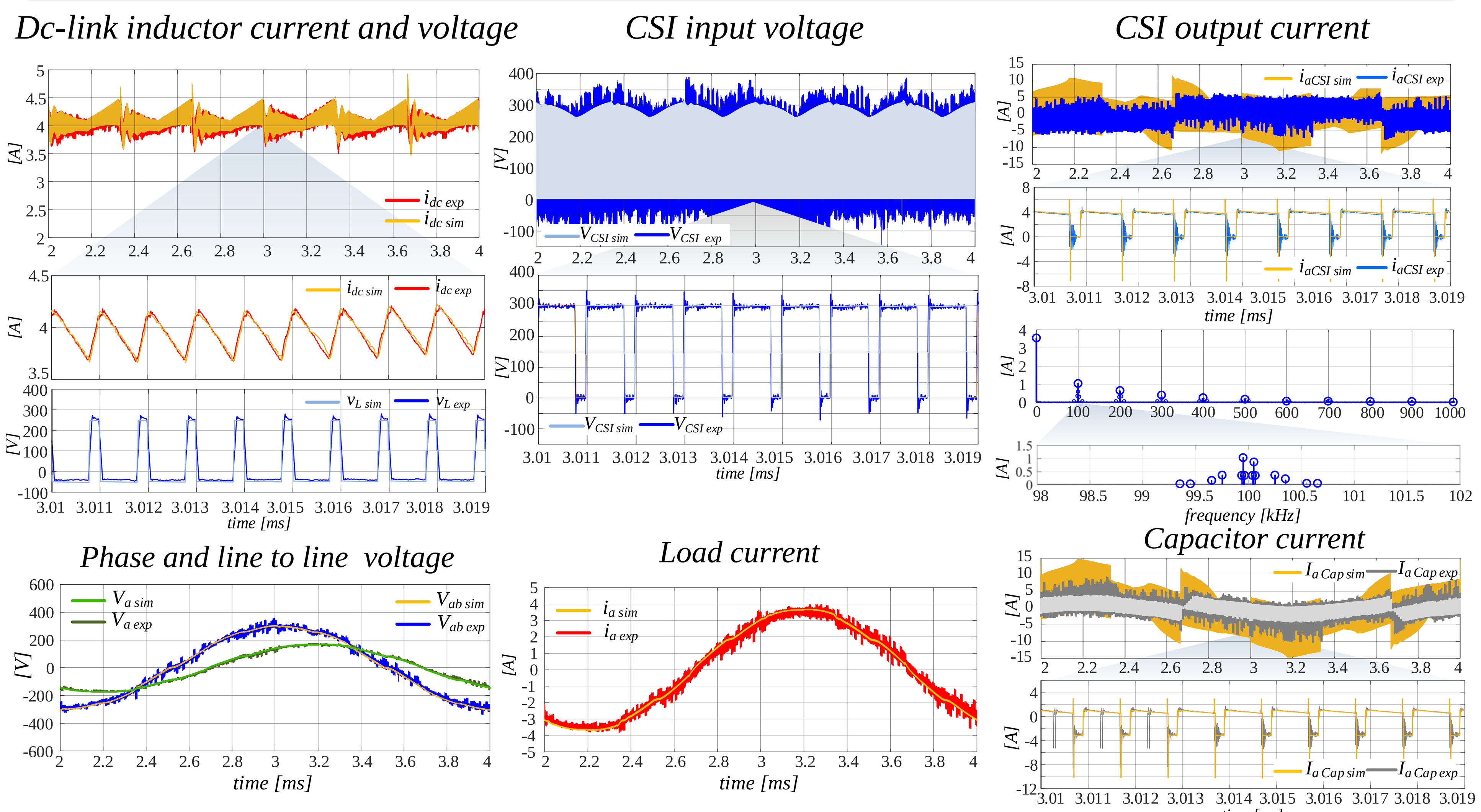

CASE 2 – PF=0.73

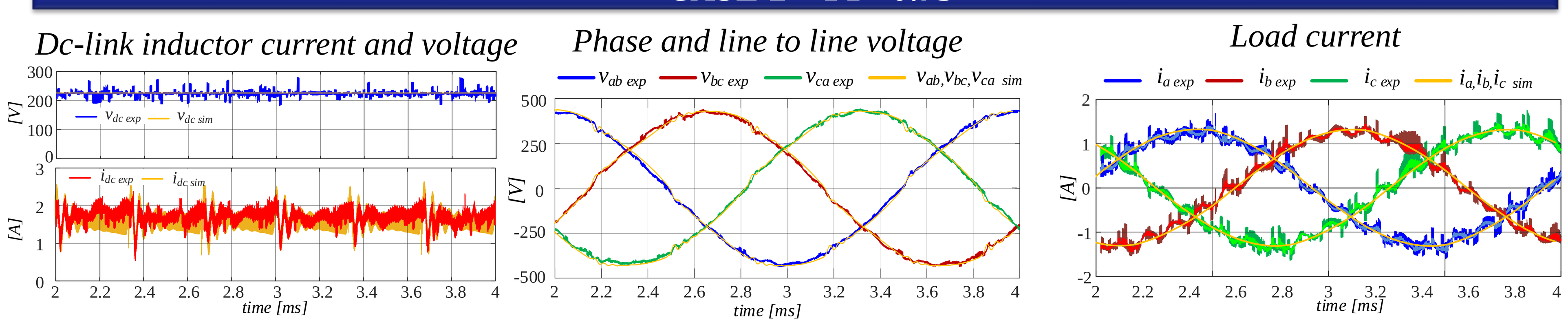

Efficiency is assessed by considering the passive components, including inductor and filter capacitor losses.

The input and output power of the CSI in steady-state is evaluated as follows:

$$P_{in}=V_{dc}\,I_{dc}$$

$$P_{out}= 3\;V_{ph}\;I_{load}\cos(\theta_v - \theta_i)$$

$$\eta = \frac{P_{out}}{P_{in}}$$

Table V: Efficiency estimation.

	Test 1				Test 2			
	exp	*sim*	*THD%e*	*THD%s*	*exp*	*sim*	*THD%e*	*THD%s*
PF	1	1			0.73			
I_{dc}	4 A	4 A			1.5 A	1.54A		
V_{dc}	238 V	238V			225.6 V	230V		
$v_{ab\,rms}$	209 V	214V	10.5	3.27	305.74 V	308 V	2.54	5.3
$v_{a\,rms}$	120 V	123V	8.56	3.33	176.3 V	179 V	2.58	4.6
i_a	2.5 A	2.6A	4.59	3.29	0.91 A	0.93A	9.65	2
η	0.94	0.95			0.9	0.91		

where, V_{dc} and I_{dc} represent the average dc-link voltage and current, respectively, measured at the input terminal of the dc-link inductor. Additionally, V_{ph} is the rms value of the fundamental component of the phase voltage, while I_{load} is the rms value of the fundamental component of the load current, θ_v and θ_i are the load voltage and current angles, respectively. The evaluated simulated and experimental efficiency for this test is listed Tab. V.

Conclusion

This work presents the modelling, simulation and experimental analysis of a current source inverter implemented with Silicon Carbide power devices. The simulation aims to replicate real behaviour through the use of behavioural models of MOSFETs and diodes, as well as accounting for parasitic elements of the passives elements. Experimental tests have confirmed the accuracy of the simulation results.